

UNIVERSITY OF BIRMINGHAM

University of Birmingham
Research at Birmingham

Poly(Sarcosine)-Based Nano-Objects with Multi-Protease Resistance by Aqueous Photoinitiated Polymerization-Induced Self-Assembly (Photo-PISA)

Varlas, Spyridon; Georgiou, Panagiotis G; Bilalis, Panayiotis; Jones, Joseph R; Hadjichristidis, Nikos; O'Reilly, Rachel K

DOI:

[10.1021/acs.biomac.8b01326](https://doi.org/10.1021/acs.biomac.8b01326)

License:

Other (please specify with Rights Statement)

Document Version

Peer reviewed version

Citation for published version (Harvard):

Varlas, S, Georgiou, PG, Bilalis, P, Jones, JR, Hadjichristidis, N & O'Reilly, RK 2018, 'Poly(Sarcosine)-Based Nano-Objects with Multi-Protease Resistance by Aqueous Photoinitiated Polymerization-Induced Self-Assembly (Photo-PISA)', *Biomacromolecules*. <https://doi.org/10.1021/acs.biomac.8b01326>

[Link to publication on Research at Birmingham portal](#)

Publisher Rights Statement:

This document is the unedited Author's version of a Submitted Work that was subsequently accepted for publication in *Biomacromolecules*, copyright © American Chemical Society after peer review. To access the final edited and published work see [10.1021/acs.biomac.8b01326](https://doi.org/10.1021/acs.biomac.8b01326)

General rights

Unless a licence is specified above, all rights (including copyright and moral rights) in this document are retained by the authors and/or the copyright holders. The express permission of the copyright holder must be obtained for any use of this material other than for purposes permitted by law.

- Users may freely distribute the URL that is used to identify this publication.
- Users may download and/or print one copy of the publication from the University of Birmingham research portal for the purpose of private study or non-commercial research.
- User may use extracts from the document in line with the concept of 'fair dealing' under the Copyright, Designs and Patents Act 1988 (?)
- Users may not further distribute the material nor use it for the purposes of commercial gain.

Where a licence is displayed above, please note the terms and conditions of the licence govern your use of this document.

When citing, please reference the published version.

Take down policy

While the University of Birmingham exercises care and attention in making items available there are rare occasions when an item has been uploaded in error or has been deemed to be commercially or otherwise sensitive.

If you believe that this is the case for this document, please contact UBIRA@lists.bham.ac.uk providing details and we will remove access to the work immediately and investigate.

Article

Poly(Sarcosine)-Based Nano-Objects with Multi-Protease Resistance by Aqueous Photoinitiated Polymerization-Induced Self-Assembly (Photo-PISA)Spyridon Varlas, Panagiotis G. Georgiou, Panayiotis Bilalis,
Joseph R. Jones, Nikos Hadjichristidis, and Rachel K. O'Reilly*Biomacromolecules*, **Just Accepted Manuscript** • DOI: 10.1021/acs.biomac.8b01326 • Publication Date (Web): 23 Oct 2018Downloaded from <http://pubs.acs.org> on October 29, 2018**Just Accepted**

"Just Accepted" manuscripts have been peer-reviewed and accepted for publication. They are posted online prior to technical editing, formatting for publication and author proofing. The American Chemical Society provides "Just Accepted" as a service to the research community to expedite the dissemination of scientific material as soon as possible after acceptance. "Just Accepted" manuscripts appear in full in PDF format accompanied by an HTML abstract. "Just Accepted" manuscripts have been fully peer reviewed, but should not be considered the official version of record. They are citable by the Digital Object Identifier (DOI®). "Just Accepted" is an optional service offered to authors. Therefore, the "Just Accepted" Web site may not include all articles that will be published in the journal. After a manuscript is technically edited and formatted, it will be removed from the "Just Accepted" Web site and published as an ASAP article. Note that technical editing may introduce minor changes to the manuscript text and/or graphics which could affect content, and all legal disclaimers and ethical guidelines that apply to the journal pertain. ACS cannot be held responsible for errors or consequences arising from the use of information contained in these "Just Accepted" manuscripts.



1
2
3
4 Poly(Sarcosine)-Based Nano-Objects with Multi-
5
6
7
8
9 Protease Resistance by Aqueous Photoinitiated
10
11
12
13 Polymerization-Induced Self-Assembly (Photo-
14
15
16
17 PISA)
18
19
20
21
22

23 *Spyridon Varlas,^a Panagiotis G. Georgiou,^{a,b} Panayiotis Bilalis,^c Joseph R. Jones,^a Nikos*
24 *Hadjichristidis,^{c*} and Rachel K. O'Reilly^{a*}*
25
26
27

28
29 ^a School of Chemistry, University of Birmingham, B15 2TT, Birmingham, UK

30
31 ^b Department of Chemistry, University of Warwick, Gibbet Hill Road, CV4 7AL, Coventry, UK

32
33 ^c Physical Sciences and Engineering Division, KAUST Catalysis Center, Polymer Synthesis
34 Laboratory, King Abdullah University of Science and Technology (KAUST), 23955, Thuwal,
35 Saudi Arabia
36
37
38

39
40 **Corresponding Authors:* nikolaos.hadjichristidis@kaust.edu.sa (N.H.) and
41 r.oreilly@bham.ac.uk (R.K.O.R.)
42
43
44
45

46 KEYWORDS

47
48 polymerization-induced self-assembly (PISA), ring-opening polymerization (ROP), reversible
49 addition-fragmentation chain-transfer (RAFT) polymerization, photoinitiated polymerization,
50
51 poly(sarcosine), protease resistance.
52
53
54
55
56
57
58
59
60

1
2
3 ABSTRACT
4
5
6

7 Poly(sarcosine) (PSar) is a non-ionic hydrophilic poly(peptoid) with numerous biologically
8 relevant properties, making it an appealing candidate for the development of amphiphilic block
9 copolymer nanostructures. In this work, the fabrication of poly(sarcosine)-based diblock
10 copolymer nano-objects with various morphologies *via* aqueous reversible addition-fragmentation
11 chain-transfer (RAFT)-mediated photoinitiated polymerization-induced self-assembly (photo-
12 PISA) is reported. Poly(sarcosine) was first synthesized *via* ring-opening polymerization (ROP)
13 of sarcosine *N*-carboxyanhydride, using high-vacuum techniques. A small molecule chain transfer
14 agent (CTA) was then coupled to the active ω -amino chain end of the telechelic polymer for the
15 synthesis of a poly(sarcosine)-based macro-CTA. Controlled chain-extensions of a commercially
16 available water-miscible methacrylate monomer (2-hydroxypropyl methacrylate) were achieved
17 *via* photo-PISA under mild reaction conditions, using PSar macro-CTA. Upon varying the degree
18 of polymerization and concentration of the core-forming monomer, morphologies evolving from
19 spherical micelles to worm-like micelles and vesicles were accessed, as determined by dynamic
20 light scattering and transmission electron microscopy, resulting in the construction of a detailed
21 phase diagram. The resistance of both colloiddally stable empty vesicles and enzyme-loaded
22 nanoreactors against degradation by a series of proteases was finally assessed. Overall, our
23 findings underline the potential of poly(sarcosine) as an alternative corona-forming polymer to
24 poly(ethylene glycol)-based analogues of PISA assemblies for use in various pharmaceutical and
25 biomedical applications.
26
27
28
29
30
31
32
33
34
35
36
37
38
39
40
41
42
43
44
45
46
47
48
49
50
51
52
53
54
55
56
57
58
59
60

INTRODUCTION

In modern polymer and materials science, poly(ethylene glycol) (PEG) and ethylene glycol-based polymers mainly from meth(acrylate) monomers are considered the gold standard for the design of nanostructures and materials with “stealth-like” properties.¹⁻³ PEG is widely utilized in various biotechnological applications such as drug/protein delivery and targeted diagnostics,^{4, 5} surface coatings,⁶ household and personal care products,^{7, 8} and cell cryopreservation.⁹ This is mainly attributed to the high flexibility and hydrophilicity, low cellular toxicity and biocompatible character of PEG that make it an efficient material for such applications.¹⁰ However, PEG is known to be a non-bio-based and non-biodegradable polymer with limited functionality, while studies have also shown oxidative activity of PEG in physiological cellular environments, immune response of patients and accelerated blood clearance phenomena caused by anti-PEG antibodies.¹¹⁻¹⁴ Consequently, in recent years there is a growing demand for finding alternatives to overcome these limitations of PEG.¹⁵

A broad variety of hydrophilic polymers including poly(glycerols),¹⁶ poly(oxazolines),¹⁷ poly(peptides)¹⁸ and poly(peptoids)¹⁹ with comparable physicochemical properties to PEG have been currently explored and proposed as promising alternatives. Among them, poly(peptoids), an important family of biomaterials, only recently have attracted the attention of scientific community.^{19, 20} Poly(sarcosine) (PSar), also referred as poly(*N*-methylated glycine), is the simplest member of the poly(peptoid) family that displays PEG-like properties and is based on an achiral endogenous but non-proteinogenic amino acid, sarcosine, mainly found in muscle tissues.^{21, 22} N-Substitution of amino acid residues in poly(peptoids) is a common synthetic procedure to promote the random coil conformation over other secondary structures (e.g. α -helices

1
2
3 and β -sheets) and to confer substantial flexibility to the polymer chains thus enhancing the
4
5 resistance of the derived materials toward enzymatic degradation.^{20, 23} PSar is a non-ionic,
6
7 hydrophilic, highly biocompatible and potentially biodegradable polymer that exhibits low cellular
8
9 toxicity, limited interactions with blood components and “stealth-like” non-immunogenic
10
11 character.^{23, 24} In addition to aqueous solubility, PSar is also highly soluble in common polar
12
13 organic solvents. Moreover, PSar can be synthesized *via* living ring-opening polymerization
14
15 (ROP) of the corresponding *N*-carboxyanhydride (NCA) to produce well-defined telechelic homo-
16
17 and copolymers with low dispersities.^{25, 26} Further post-polymerization modification of the living
18
19 amino-terminal chain end allows for the insertion of various functionalities and the combination
20
21 of PSar with other synthetic polymers. Overall, the unique features of PSar suggest that it can be
22
23 effectively utilized as a PEG-alternative corona-forming block imparting higher colloidal stability
24
25 (i.e. prevention of protein-induced aggregation), minimal systemic toxicity and longer circulation
26
27 times *in vivo* to amphiphilic block copolymer assemblies.²³
28
29
30
31
32
33

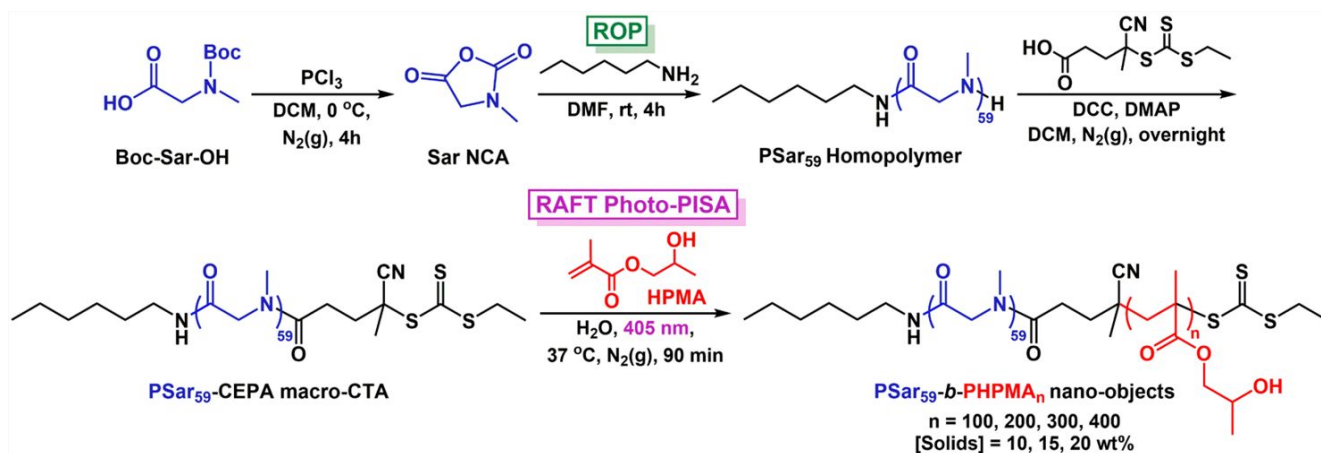
34 Over the last years, studies on the synthesis and self-assembly behavior of PSar-based block
35
36 copolymers for the development of nanostructures of biotechnological interest have been
37
38 presented, although they involve the use of conventional self-assembly procedures in dilute
39
40 aqueous solutions.^{13, 23, 27-32} Recently, polymerization-induced self-assembly (PISA) has
41
42 been established as an efficient methodology for facile one-pot fabrication of polymeric
43
44 nano-objects with predictable morphologies at high solids concentrations (10-50% w/w).³³⁻
45
46 ³⁶ Existing limitations of traditional self-assembly strategies (i.e. direct dissolution, thin-
47
48 film hydration, and solvent-switch) such as low polymer concentrations ($\leq 1\%$ w/w) and
49
50 laborious post-polymerization processing steps for targeting certain morphologies are
51
52 proven to be overcome by PISA. Only selected monomers have the ability to undergo PISA
53
54
55
56
57
58
59
60

1
2
3 since a solubility transition of the gradually growing core-forming block from solvent-
4 soluble to solvent-immiscible is required.³⁴ In principle, PISA can be achieved by using
5
6 any known polymerization technique, although the vast majority of PISA studies to date
7
8 involve implementation of reversible-deactivation radical polymerization (RDRP)
9
10 techniques, including atom transfer radical polymerization (ATRP),^{37, 38} nitroxide-
11
12 mediated polymerization (NMP),^{39, 40} and reversible addition-fragmentation chain-transfer
13
14 (RAFT) polymerization,⁴¹⁻⁴⁴ under either dispersion or emulsion polymerization
15
16 conditions, owing to their versatility and broad applicability. Ring-opening metathesis
17
18 polymerization (ROMP) has been also introduced lately as a non-radical approach for PISA
19
20 in both aqueous and organic media.⁴⁵⁻⁴⁷
21
22
23
24
25
26

27 In particular, there has been rapidly growing research interest in aqueous RAFT-mediated
28
29 photoinitiated PISA (photo-PISA) *via* either the well-described “photoiniferter”
30
31 mechanism of chain transfer agents (CTAs) or by using special photoinitiators and
32
33 photoredox catalysts under ultraviolet or visible-light irradiation.^{42, 48-54} This is mainly
34
35 attributed to the ambient temperatures and mild reaction conditions of photo-PISA that are
36
37 not harmful to sensitive biomolecules (i.e. drugs, enzymes, membrane proteins) enabling
38
39 their direct encapsulation into well-defined polymeric vesicles for the one-pot development
40
41 of cargo-loaded delivery vehicles and nanoreactors of further bio-related interest.⁵⁵⁻⁵⁹
42
43
44
45

46 Herein, the preparation of diblock copolymer nano-objects with different morphologies bearing
47
48 a PSar hydrophilic corona *via* a combination of NCA ROP and RAFT-mediated photo-PISA is
49
50 reported. First, sarcosine NCA (Sar NCA) was synthesized from the corresponding *N*-Boc-
51
52 protected amino acid. Living ROP of Sar NCA using high-vacuum techniques and an amino
53
54 initiator yielded an ω -telechelic PSar homopolymer with monomodal molecular weight
55
56
57
58
59
60

distribution and low dispersity (D_M). Due to the absence of side chain functional groups found in poly(peptides), quantitative coupling between an acid-functionalized small molecule CTA and the sterically accessible N-terminus of PSar was achieved, resulting in the formation of a water-soluble PSar macromolecular CTA (macro-CTA). As a next step, PSar macro-CTA was used to carry out aqueous photo-PISA reactions of 2-hydroxypropyl methacrylate (HPMA) under dispersion polymerization conditions by varying PHPMA degrees of polymerization and total solids concentration (Scheme 1). The obtained PSar-*b*-PHPMA diblock copolymer assemblies were characterized by dynamic light scattering (DLS), zeta-potential analysis and transmission electron microscopy (TEM) imaging, resulting in the construction of a morphologies diagram. To further explore the robust nature and PEG-like characteristics of PSar-based nano-objects, the colloidal stability of PSar-*b*-PHPMA unilamellar vesicles in physiological media and the effect of a series of typical proteolytic enzymes (i.e. α -chymotrypsin, trypsin and pepsin) on empty and protein-loaded vesicles were evaluated revealing the great potential of such materials for biomedical applications.



Scheme 1. Schematic illustration of the synthetic route followed for the synthesis of PSar₅₉-*b*-PHPMA_n ($n = 100, 200, 300,$ and 400) diblock copolymer nano-objects at $[\text{solids}] = 10, 15,$ and $20\text{ wt}\%$ via aqueous RAFT-mediated photo-PISA, using a PSar₅₉-based macro-CTA.

EXPERIMENTAL SECTION

Materials and methods

Materials and characterization techniques used are given in detail in the Supporting Information (SI).

Synthetic Procedures

Synthesis of sarcosine *N*-carboxyanhydride (Sar NCA). Boc-*N*-methylglycine (Boc-Sar-OH) (7.0 g, 0.037 mol) was added into a three-neck round-bottom flask and degassed under vacuum overnight. Then, 300 mL of dry DCM was distilled and the solution was left under stirring for 30 min at 0 °C. Subsequently, phosphorous trichloride (PCl₃) (4.0 mL, 0.046 mol) was diluted into 30 mL of dry DCM, added dropwise to the flask *via* a dropping funnel and the reaction was left to proceed for 4 h at 0 °C under nitrogen atmosphere. The solvent and the volatiles were removed under reduced pressure, yielding a yellowish oil as the crude reaction product. The crude product was then sublimated at 70 °C under high vacuum (10⁻⁵ mbar) resulting in the formation of Sar NCA crystals (3.1 g, 0.027 mol, 73%, m. p.: 103–104 °C (lit.: 102–105 °C)).⁶⁰ ¹H-NMR (400 MHz, DMSO-*d*₆): δ (ppm) 4.23 (s, 2H, **CH**₂), 2.87 (s, 3H, **CH**₃). FT-IR (neat): ν (cm⁻¹) 1848, 1761 (C=O).

Synthesis of 4-cyano-4-[(ethylsulfanylthiocarbonyl)sulfanyl] pentanoic acid (CEPA). A previously described process was followed for the synthesis of 4-cyano-4-[(ethylsulfanylthiocarbonyl)sulfanyl] pentanoic acid chain transfer agent (CEPA CTA).⁶¹ In

1
2
3 particular, sodium ethanethiolate (10.0 g, 0.119 mol, 1 eq) was suspended in 500 mL of dry diethyl
4 ether at 0 °C. Carbon disulfide (7.74 mL, 0.131 mol, 1.1 eq) was subsequently added dropwise
5
6 over 10 min, resulting to the formation of a thick yellow precipitate of sodium *S*-ethyl
7
8 trithiocarbonate. After 2 h of stirring at room temperature, solid iodine (15.1 g, 0.059 mol, 0.5 eq)
9
10 was added to the reaction medium. After 2 h, the solution was washed three times with aqueous
11
12 sodium thiosulfate (1 M), water and finally saturated NaCl solution. The organic layer was
13
14 thoroughly dried over MgSO₄ and the crude bis-(ethylsulfanylthiocarbonyl) disulfide was then
15
16 isolated by rotary evaporation (16.2 g, 0.059 mol).
17
18

19
20 A solution of bis-(ethylsulfanylthiocarbonyl) disulfide (16.2 g, 0.059 mol, 1 eq) and 4,4'-azobis(4-
21
22 cyanopentanoic acid) (ACVA) (24.8 g, 0.0885 mol, 1.5 eq) in 500 mL ethyl acetate was heated at
23
24 reflux for 18 h under N₂(g) atmosphere. Following rotary evaporation of the solvent, the crude
25
26 CEPA CTA was isolated by flash column chromatography using silica gel as the stationary phase
27
28 and 75:25 DCM-petroleum ether as the eluent. The isolated product was precipitated out of
29
30 solution using hexane, leaving a yellow-light orange solid. The final product was collected and
31
32 dried under reduced pressure to afford pure CEPA CTA (21.36 g, 0.081 mol, 69%). ¹H-NMR (400
33
34 MHz, CDCl₃): δ (ppm) 3.35 (q, 2H, S-CH₂-CH₃), 2.38-2.71 (m, 4H, CH₂-CH₂), 1.89 (s, 3H,
35
36 C(CN)-CH₃), 1.36 (t, 3H, S-CH₂-CH₃). ¹³C-NMR (100 MHz, CDCl₃): δ (ppm) 217.0, 177.2,
37
38 119.2, 46.5, 33.5, 31.7, 29.5, 25.0, 12.9. FT-IR (neat): ν (cm⁻¹) 2235 (C≡N), 1709 (C=O), 1073
39
40 (C=S). HRMS: m/z [C₉H₁₃NO₂S₃+Na]⁺ calc. 286.0001 g mol⁻¹, exp. 286.0001 g mol⁻¹.
41
42
43
44
45
46
47
48
49

50 **Synthesis of poly(sarcosine)₅₉ (PSar₅₉) via ring-opening polymerization (ROP) of Sar NCA.**

51
52 In a flame-dried round bottom flask, n-hexylamine (0.048 mL, 3.6×10⁻⁵ mol) was added, followed
53
54 by distillation of 30 mL highly pure DMF. The flask was transferred to the glove box and a 10 mL
55
56
57
58
59
60

1
2
3 solution of Sar NCA (2.9 g, 0.0252 mol) in DMF was added and the solution was vigorously stirred
4
5 at room temperature. Periodically, the solution was pumped to remove the CO₂ (g) produced
6
7 during polymerization. The consumption of Sar NCA was monitored by FT-IR spectroscopy
8
9 through removal of an aliquot of the solution in the glove box. Upon completion of the
10
11 polymerization reaction (4 h), the final PSar homopolymer was precipitated in diethyl ether and
12
13 dried under vacuum overnight (1.5 g, 83%). ¹H-NMR (400 MHz, D₂O): δ (ppm) 4.49-4.05 (br m,
14
15 CH₂ of PSar backbone), 3.21 (m, 2H, CH₂-CH₂-NH), 3.10-2.81 (br m, CH₃ of PSar side chain),
16
17 1.50 (s, 2H, (CH₂)₃-CH₂-CH₂-NH), 1.29 (s, 6H, CH₃-(CH₂)₃-CH₂), 0.86 (s, 3H, CH₃-(CH₂)₃-CH₂).
18
19 $M_{n, NMR} = 4,200 \text{ g mol}^{-1}$ ($DP_{PSar, NMR} = 59$). FT-IR (neat): ν (cm⁻¹) 1641 (C=O of amide). SEC (5
20
21 mM NH₄BF₄ in DMF) $M_{n, SEC RI} = 7,700 \text{ g mol}^{-1}$, $D_{M, SEC RI} = 1.08$. $M_{w, SLS} = 5,500 \text{ g mol}^{-1}$.
22
23
24
25
26
27
28

29 **Synthesis of poly(sarcosine)₅₉-CEPA macro-CTA (PSar₅₉-CEPA macro-CTA).** PSar₅₉-CEPA
30
31 macro-CTA was synthesized by dicyclohexylcarbodiimide (DCC) coupling between PSar₅₉ and
32
33 CEPA CTA according to previously reported methods.^{42, 48, 59} Poly(sarcosine) homopolymer ($M_{n,$
34
35 $NMR} = 4,200 \text{ g mol}^{-1}$, PSar₅₉) (1 g, 2.4×10^{-4} mol, 1 eq) was dissolved in 20 mL of dry DCM. The
36
37 resulting solution was then purged with N₂ (g) for 30 min. After complete dissolution, CEPA CTA
38
39 (0.253 g, 9.6×10^{-4} mol, 4 eq), DCC (99 mg, 4.8×10^{-4} mol, 2 eq) and DMAP (5.9 mg, 4.8×10^{-5} mol,
40
41 0.2 eq) were added to the reaction mixture. The amide formation reaction proceeded with stirring
42
43 at room temperature for 18 h under continuous N₂ (g) flow. After this period, DCC (99 mg, 4.8×10^{-4}
44
45 mol, 2 eq) and DMAP (5.9 mg, 4.8×10^{-5} mol, 0.2 eq) were added for a second time to the reaction
46
47 mixture and then stirred at room temperature for an additional period of 6 h under continuous N₂
48
49 (g) flow. The solution was then filtered to remove unreacted DCC and DMAP. Following rotary
50
51 evaporation of DCM, the resulted PSar₅₉-CEPA macro-CTA was collected by precipitation into
52
53
54
55
56
57
58
59
60

1
2
3 250 mL of cold diethyl ether, redissolved in deionized water (DI) and dialyzed against DI water
4
5 for 48 h (dialysis membrane MWCO = 1,000 Da). The purified PSar₅₉-CEPA macro-CTA was
6
7 then lyophilized to give a yellowish solid as the final product (0.82 g, 1.8×10^{-4} mol, 76%). ¹H-
8
9 NMR (400 MHz, CDCl₃): δ (ppm) 4.35-3.85 (br m, CH₂ of PSar backbone), 3.35 (q, 2H, CH₃-
10
11 CH₂-S-(C=S)), 3.21 (m, 2H, CH₂-CH₂-NH), 3.10-2.85 (br m, CH₃ of PSar side chain), 2.69 (m,
12
13 2H, CH₂-(C=O)-N-CH₃), 2.52-2.35 (m, 2H, C(CN)-CH₂), 1.91 (s, 3H, CH₃-C-(CN)), 1.49 (s, 2H,
14
15 (CH₂)₃-CH₂-CH₂-NH), 1.36 (t, 3H, CH₃-CH₂-S-(C=S)), 1.25 (d, 6H, CH₃-(CH₂)₃-CH₂), 0.88 (s,
16
17 3H, CH₃-(CH₂)₃-CH₂). SEC (5 mM NH₄BF₄ in DMF) $M_{n, SEC RI} = 8,300 \text{ g mol}^{-1}$, $D_{M, SEC RI} = 1.09$.
18
19
20
21
22
23

24 **Synthesis of PSar₅₉-*b*-PHPMA_n diblock copolymer nano-objects by aqueous RAFT-mediated**

25 **photoinitiated polymerization-induced self-assembly (photo-PISA).** All photo-PISA reactions

26
27 were performed in a custom-built photoreactor setup (see the Supporting Information for details).
28
29

30 This ensured the polymerization solutions were only exposed to the light from the 400–410 nm
31
32

33 LED source placed underneath the vials (radiant flux of 800 mW@400 mA). A typical synthetic
34
35

36 procedure to achieve PSar₅₉-*b*-PHPMA₂₀₀ diblock copolymer nano-objects at 15 wt% solids
37
38

39 content by aqueous RAFT-mediated photo-PISA is described.^{42, 59} PSar₅₉-CEPA mCTA (20 mg,
40
41

42 4.4×10^{-6} mol, 1 eq) and HPMA (128 mg, 8.9×10^{-4} mol, 200 eq) were dissolved in deionized water
43
44

45 (0.84 mL) in a sealed 15 mL scintillation vial bearing a magnetic stirrer bar. The resulting
46
47

48 polymerization solution was degassed by purging with N₂ (g) for 15 min. The sealed vial was
49
50

51 incubated at 37 °C with magnetic stirring under 405 nm light irradiation for 90 min to ensure full
52
53

54 monomer conversion. After this period, the reaction mixture was exposed to air and allowed to
55
56

57 cool to room temperature. The resulting solution of particles was then diluted ten-fold in DI water
58
59

60 and purified by three centrifugation/resuspension cycles in DI water at 14000 rpm. ¹H-NMR in

1
2
3 methanol- d_4 and DMF SEC analyses of the pure copolymers were performed after lyophilization
4 of an aliquot of particles. TEM, DLS and zeta potential analyses were performed on samples after
5 dilution to an appropriate analysis concentration. $^1\text{H-NMR}$ (400 MHz, CD_3OD): δ (ppm) 5.60 (br
6 s, OH), 4.47-4.10 (br m, CH_2 of PSar backbone), 4.03 and 3.88 (br s, CH and CH_2 of PHPMA
7 side chain), 3.63 (br s, CH of PHPMA side chain, isomer peak), 3.10-2.89 (br m, CH_3 of PSar side
8 chain), 2.23-1.75 (br m, CH_2 of PHPMA backbone), 1.50-0.75 (br m, CH_3 of PHPMA backbone
9 and CH_3 of PHPMA side chain).
10
11
12
13
14
15
16
17
18
19
20
21

22 **Encapsulation of HRP into PSar₅₉-*b*-PHPMA₄₀₀ vesicles by one-pot aqueous RAFT photo-**
23 **PISA.** For the preparation of HRP-loaded PSar₅₉-*b*-PHPMA₄₀₀ vesicles by aqueous photo-PISA at
24 10 wt% solids content, a typical synthetic protocol was followed.⁵⁷ PSar₅₉-CEPA mCTA (10 mg,
25 2.2×10^{-6} mol, 1 eq) and HPMA (128 mg, 8.9×10^{-4} mol, 400 eq) were dissolved in deionized water
26 (1.14 mL) in a sealed 15 mL scintillation vial bearing a magnetic stirrer bar. Once homogeneous,
27 0.1 mL of a 200 U mL⁻¹ HRP solution in DI water was added. The resulting polymerization
28 solution was degassed by purging with N_2 (g) for 15 min. The sealed vial was incubated at 37 °C
29 with magnetic stirring under 405 nm light irradiation for 90 min to ensure full monomer
30 conversion. After this period, the reaction mixture was exposed to air and allowed to cool to room
31 temperature. The resulting solution of particles was then diluted ten-fold in 100 mM PB (pH = 7.0)
32 and purified by five centrifugation/resuspension cycles in 100 mM PB (pH = 7.0) at 14000 rpm
33 for the removal of unreacted monomer and free HRP enzyme.
34
35
36
37
38
39
40
41
42
43
44
45
46
47
48
49
50
51
52

53 **Incubation of empty and HRP-loaded PSar₅₉-*b*-PHPMA₄₀₀ vesicles with different proteolytic**
54 **enzymes (proteases).** Empty PSar₅₉-*b*-PHPMA₄₀₀ vesicles purified in 100 mM phosphate buffer
55
56
57
58
59
60

(PB) (pH = 7.0 for a-chymotrypsin and trypsin or pH = 1.8 for pepsin) at 10× dilution (1 wt% solids content) (2 mL) were incubated with either 25 mg mL⁻¹ a-CT (pH = 7.0), 25 mg mL⁻¹ trypsin (pH = 7.0) or 25 mg mL⁻¹ pepsin (pH = 1.8) solutions (0.2 mL) at 37 °C. Aliquots were taken over a period of 72 h and samples were analyzed by DLS, DMF SEC and dry-state TEM imaging to determine the effect of different proteases on the characteristics of particles.

HRP-loaded PSar₅₉-*b*-PHPMA₄₀₀ vesicles purified in 100 mM PB (pH = 7.0 for a-CT and trypsin) at 10× dilution (1 wt% solids content) (2 mL) were incubated with either 100 mM PB (pH = 7.0), 25 mg mL⁻¹ a-CT or trypsin (pH = 7.0) solutions (0.2 mL) at 37 °C for a period of 72 h. Aliquots were taken at 18 h and 72 h and the relative activities of particles were assessed by kinetic colorimetric analysis using a plate reader. For the free HRP, 2 U mL⁻¹ solutions in 100 mM PB (pH = 7.0) (2 mL) were incubated with either 100 mM PB (pH = 7.0), 25 mg mL⁻¹ a-CT or trypsin (pH = 7.0) solutions (0.2 mL) at 37 °C for a period of 72 h. Aliquots were taken at 18 h and 72 h and the relative activities of free HRP solutions were assessed in an identical manner. Pepsin was not used in case of HRP-loaded vesicles due to significant difference in optimum pH range of the two enzymes.

Kinetic colorimetric analyses for determination of activity of HRP-loaded PSar₅₉-*b*-PHPMA₄₀₀ vesicles in presence of different proteases. Purified HRP-loaded PSar₅₉-*b*-PHPMA₄₀₀ vesicles incubated with either PB, a-CT or trypsin at 20× dilution (0.5 wt% solids content) in 100 mM PB (pH = 7.0) (120 μL) were diluted with 100 mM PB (pH = 7.0) (40 μL) in a 96-well plate microwell. *O*-dianisidine (4 mM, 20 μL) was then added. Finally, a 35 wt% aqueous solution of hydrogen peroxide (20 μL) was added and the change in absorbance at λ = 492 nm was recorded every minute for a period of 60 min using a plate reader. In a similar process, the free

1
2
3 HRP solutions incubated with either PB, a-CT or trypsin at 1 U mL^{-1} in $100 \text{ mM PB (pH = 7.0)}$
4
5 $(20 \text{ }\mu\text{L})$ were diluted with $100 \text{ mM PB (pH = 7.0)}$ $(140 \text{ }\mu\text{L})$ in a 96-well plate microwell. *O*-
6
7 dianisidine $(4 \text{ mM}, 20 \text{ }\mu\text{L})$ was then added. Finally, a $35 \text{ wt}\%$ aqueous solution of hydrogen
8
9 peroxide $(20 \text{ }\mu\text{L})$ was added and the change in absorbance was monitored in an identical manner.
10
11
12 All measurements were performed in quadruplicate.
13
14
15
16

17 **Colloidal stability studies of PSar₅₉-*b*-PHPMA₄₀₀ vesicles in physiological media.** To assess
18
19 the colloidal stability of empty PSar₅₉-*b*-PHPMA₄₀₀ vesicles (prepared at $[\text{solids}] = 10 \text{ wt}\%$) and
20
21 their interaction with complex physiological media, a typical protocol was followed.⁶² FBS and
22
23 cell growth medium were first incubated at $37 \text{ }^\circ\text{C}$ for 15 min. Purified PSar₅₉-*b*-PHPMA₄₀₀ vesicles
24
25 were suspended in DI water at a final concentration of $1 \text{ wt}\%$ prior to mixing with FBS or cell
26
27 growth medium. Then, $80 \text{ }\mu\text{L}$ of $1 \text{ wt}\%$ vesicles were dispersed in either 10 mL DI water or cell
28
29 growth medium or 10 mL of $1:9 \text{ FBS:DI H}_2\text{O}$ solution, with gentle agitation. The resulting particle
30
31 solutions were incubated at $37 \text{ }^\circ\text{C}$ and D_h changes of vesicles were monitored by DLS over a period
32
33 of 72 h.
34
35
36
37
38
39

40 RESULTS AND DISCUSSION

41
42 **Synthesis and characterization of poly(sarcosine)₅₉ (PSar₅₉) homopolymer.** The first
43
44 step for the preparation of PSar homopolymer involved the synthesis of the corresponding
45
46 *N*-carboxyanhydride of sarcosine (Sar NCA). This was achieved by cyclization reaction of
47
48 *N*-Boc-protected sarcosine using PCl_3 as chlorinating agent for the formation of Sar NCA
49
50 ring molecule (Scheme 1). The reaction was completed in 4 h as evidenced by FT-IR
51
52 spectroscopy (Figure S2, SI). The appearance of two characteristic peaks at 1761 and 1848
53
54
55
56
57
58
59
60

1
2
3 cm⁻¹ are indicative of the $\nu(\text{C}=\text{O})$ vibrations of the Sar NCA ring. The crude product was
4 purified by sublimation *in vacuo* resulting in the formation of Sar NCA crystals. The
5
6 successful synthesis and purification of Sar NCA was confirmed by ¹H-NMR spectroscopy
7
8 in DMSO-*d*₆ (Figure S1A, SI). Although the “Fuchs-Farthing” method is considered the
9
10 standard approach for the synthesis of amino acid NCAs (i.e. use of phosgene or derivatives
11
12 at elevated temperatures), the alternative mild synthetic procedure followed herein resulted
13
14 in highly pure final product of Sar NCA at high yield.
15
16
17
18

19
20 Next, ω -telechelic PSar homopolymer was synthesized *via* living ring-opening
21
22 polymerization (ROP) of Sar NCA. The polymerization reaction proceeded under high
23
24 vacuum at room temperature for 4 h using n-hexylamine as the initiator and DMF as the
25
26 solvent, and was terminated by precipitation in diethylether (Scheme 1). Monitoring of the
27
28 ROP kinetics was carried out *via* FT-IR spectroscopy as evidenced by the disappearance of
29
30 the NCA peaks (1761 and 1848 cm⁻¹) and the gradual appearance of a sharp peak at 1641
31
32 cm⁻¹ attributed to the $\nu(\text{C}=\text{O})$ vibration of the formed poly(peptoid) amide bonds (Figure
33
34 S2, SI). SEC analysis in DMF with 5 mM NH₄BF₄ was carried out to get a rough molecular
35
36 weight estimate of the homopolymer as PMMA can be poor standard for PSar, while it
37
38 revealed a narrow monomodal molecular weight distribution peak of low dispersity (M_n ,
39
40 $SEC_{RI} = 7,700 \text{ g mol}^{-1}$, $D_{MRI} = 1.08$) (Figure 1B).⁶⁰ ¹H-NMR spectroscopy in D₂O was used
41
42 for the determination of the average degree of polymerization (DP) of the final purified
43
44 PSar by comparing the integral ratio of the peak corresponding to -CH₃ group of
45
46 hexylamine at 0.86 ppm ($I_{0.86 \text{ ppm}} = 3.00$) to the peak of -CH₃ groups of PSar backbone at
47
48 2.81-3.10 ppm ($I_{2.81-3.10 \text{ ppm}} = 177.25$) (ca. $DP_{PSar} = 59$, $M_{n, NMR} = 4,200 \text{ g mol}^{-1}$) (Figure S1B,
49
50 SI). Analysis of static and dynamic light scattering over a range of scattering lengths (10.7
51
52
53
54
55
56
57
58
59
60

$\leq q \leq 23.0 \mu\text{m}^{-1}$) was used to estimate the weight-average molecular weight and intensity-weighted hydrodynamic radius of PSar₅₉ in DI water ($M_w = (5.50 \pm 0.09) \times 10^3 \text{ Da}$; $\langle R_h \rangle_Z = (1.95 \pm 0.03) \text{ nm}$) (Figure S3, SI). The mutual consistency of these two measurements was then verified by reference to an empirical formula published previously by Weber et al.⁶⁰

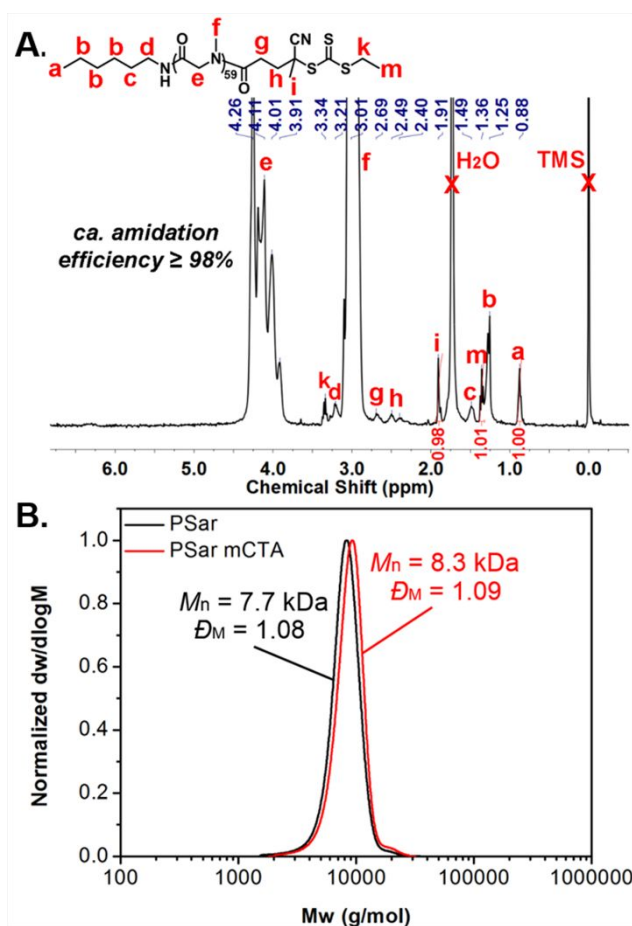


Figure 1. (A) ^1H -NMR spectrum of PSar₅₉-CEPA macro-CTA in CDCl_3 . (B) Normalized SEC RI molecular weight distributions for PSar₅₉ homopolymer (black trace) and PSar₅₉-CEPA macro-CTA (red trace), along with the corresponding M_n and D_M values. M_n and D_M values were calculated from PMMA standards using 5 mM NH_4BF_4 in DMF as the eluent.

Aqueous RAFT-mediated photoinitiated polymerization-induced self-assembly (photo-PISA) of PSar₅₉-*b*-PHPMA_n diblock copolymer nano-objects. In order to conduct aqueous RAFT-mediated photo-PISA reactions using PSar₅₉ as the hydrophilic steric stabilizer, a small molecule CTA (CEPA CTA) suitable for methacrylate monomers was introduced to the PSar chain ends to afford a PSar-based macro-CTA. This was achieved through amide bond formation between the acid-functionalized CEPA CTA and the sterically accessible amino end group of PSar by DCC coupling chemistry under dry conditions (Scheme 1). Quantitative amidation efficiency ($\geq 98\%$) was calculated from ¹H-NMR spectroscopy in chloroform-*d* by comparing the integral ratio of the peak corresponding to –CH₃ group of hexylamine at 0.88 ppm ($I_{0.88 \text{ ppm}} = 1.00$) to the peak of –CH₃ group of CTA at 1.91 ppm ($I_{1.91 \text{ ppm}} = 0.98$) (ca. amidation efficiency (%) = $(I_{1.91 \text{ ppm}}/I_{0.88 \text{ ppm}}) \times 100$, Figure 1A). Based on ¹H-NMR analysis, there is approximately 2% of non-functionalized PSar₅₉ homopolymer that is not separated from PSar₅₉-CEPA macro-CTA as they both precipitate from diethyl ether. SEC analysis of the purified and lyophilized PSar₅₉ macro-CTA in 5 mM NH₄BF₄ in DMF revealed the successful attachment of CEPA, as judged by the small increase of molecular weight compared to PSar₅₉ and the characteristic absorbance of the trithiocarbonate group of the macro-CTA peak at $\lambda = 309 \text{ nm}$ ($M_{n, \text{SEC RI}} = 8,300 \text{ g mol}^{-1}$, $D_{\text{M RI}} = 1.09$) (Figure 1B).

Subsequently, the prepared water-soluble PSar₅₉ macro-CTA was chain-extended under RAFT dispersion PISA conditions using the well-documented water-miscible monomer 2-hydroxypropyl methacrylate (HPMA) (mixture of 2-hydroxypropyl methacrylate - 75 mol % and 2-hydroxyisopropyl methacrylate – 25 mol%) for the formation of the water-insoluble core-forming block. Aqueous RAFT-mediated photo-PISA reactions of HPMA for the fabrication of PSar₅₉-*b*-PHPMA_n diblock copolymer nano-objects were carried out under 405

1
2
3 nm visible-light irradiation (radiant flux of 800 mW@400 mA) at 37 °C (N₂ atmosphere) in
4
5 the absence of a photoinitiator or catalyst (Scheme 1). As an initial step, the required photo-
6
7 PISA reaction time to ensure complete monomer conversions was determined *via* kinetic
8
9 study of a PSar₅₉-*b*-PHPMA₄₀₀ system at 10 wt% total solids content. Aliquots were
10
11 withdrawn from the polymerization mixture every 5 min and samples were analysed by ¹H-
12
13 NMR spectroscopy in methanol-*d*₄ for monomer conversion calculation and SEC analysis
14
15 using 5 mM NH₄BF₄ in DMF as the eluent. As shown in Figure 2A, the photo-PISA reaction
16
17 followed pseudo-first-order kinetics separated into two regimes with quantitative monomer
18
19 conversion (>99%) achieved after 90 min of irradiation time. Based on the semilogarithmic
20
21 plot, the first regime from 0 to 25 min corresponds to growing solvent-soluble PSar₅₉-*b*-
22
23 PHPMA_n chains, while for the second regime a significant increase in polymerization rate
24
25 typically occurring in a PISA process was observed after approximately 25 min ascribed to a
26
27 monomer conversion of 36.5% that is attributed to the onset of particle micellization resulting
28
29 in a relatively high local HPMa concentration.^{33, 63} SEC monitoring during the kinetic study
30
31 revealed the linear evolution of *M*_n values with conversion and verified the controlled
32
33 character of the photo-PISA process, while *D*_M values remained relatively low with
34
35 progression of conversion (*D*_M max = 1.50), given that a high DP of PHPMA was targeted in
36
37 this case (Figure 2B).
38
39
40
41
42
43
44
45
46
47
48
49
50
51
52
53
54
55
56
57
58
59
60

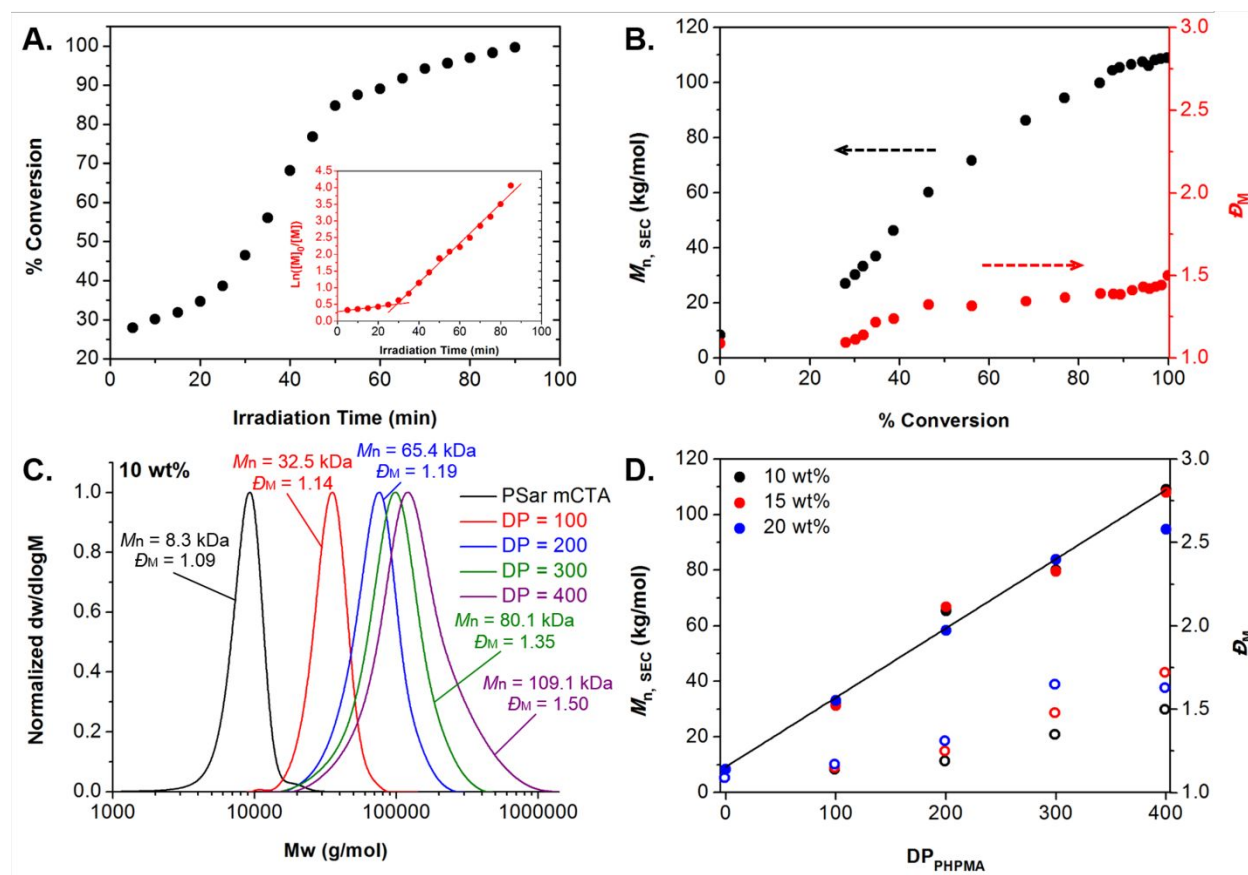


Figure 2. (A) Polymerization kinetics for aqueous RAFT-mediated photo-PISA of HPMA using PSar₅₉-CEPA as the macro-CTA at [solids] = 10 wt% (target DP_{PHPMA} = 400) (inset: $\ln([M]_0/[M])$ versus irradiation time kinetic plot). (B) Evolution of number-average molecular weight (M_n) and molar mass distribution (\mathcal{D}_M) values with monomer conversion for aqueous RAFT-mediated photo-PISA of HPMA using PSar₅₉-CEPA as the macro-CTA at [solids] = 10 wt% (target DP_{PHPMA} = 400). (C) Normalized SEC RI molecular weight distributions for PSar₅₉-CEPA macro-CTA (black trace) and PSar₅₉-*b*-PHPMA_n diblock copolymers (n = 100 - red trace, 200 - blue trace, 300 - green trace, and 400 - purple trace) at [solids] = 10 wt%, along with their corresponding M_n and \mathcal{D}_M values. (D) Evolution of M_n (filled circles) and \mathcal{D}_M (empty circles) values calculated from SEC RI analysis with increasing target DP of PHPMA for PSar₅₉-*b*-PHPMA_n diblock copolymers prepared *via* aqueous RAFT-mediated photo-PISA at [solids] = 10, 15, and 20 wt%. In all cases M_n and \mathcal{D}_M values were calculated from PMMA standards using 5 mM NH₄BF₄ in DMF as the eluent.

1
2
3 Next, a series of aqueous photo-PISA reactions under the same mild polymerization
4 conditions were carried out for 90 min for the development of PSar₅₉-*b*-PHPMA_{*n*} diblock
5 copolymer nano-objects of different morphologies by targeting various DPs of the core-
6 forming PHPMA block (DP_{PHPMA} = 100, 200, 300, and 400) and total solids concentrations
7 ([solids] = 10, 15, and 20 wt%). In all cases complete monomer conversion (≥98%) was
8 achieved in 90 min of irradiation time, as determined by ¹H-NMR spectroscopic analysis in
9 methanol-*d*₄ of the crude copolymer samples (Table S1, SI). The PSar₅₉-*b*-PHPMA_{*n*} nano-
10 object samples were purified by consecutive centrifugation-resuspension cycles in DI water
11 for the removal of unreacted monomer (Figure S4, SI). Based on SEC analysis of lyophilized
12 samples using 5 mM NH₄BF₄ in DMF as the eluent, the well-controlled character of photo-
13 PISA reactions at different solids content was revealed. Specifically, in all cases symmetrical
14 monomodal molecular weight distributions were observed shifting linearly toward higher
15 molecular weight (*M*_{*n*}) values upon increasing the DP of PHPMA with no apparent trace of
16 bimolecular termination (Figures 2C and S5, SI). Based on SEC RI chromatograms of PSar₅₉-
17 *b*-PHPMA_{*n*} diblock copolymers, a low molecular weight peak that corresponds to non-
18 separated and non-functionalized PSar₅₉ homopolymer (~4–5% of PSar₅₉-CEPA macro-CTA
19 trace in all cases, ca. 2% from ¹H-NMR analysis) is observed, but since it doesn't contribute
20 to RAFT-mediated chain-extensions of PHPMA or affect the overall nano-object
21 characteristics it was not taken into consideration for the calculation of *M*_{*n*} and *D*_{*M*} values of
22 the main PSar₅₉-*b*-PHPMA_{*n*} diblock copolymer peak in each case (Figure S6, SI).
23 Importantly, for a series of samples with specified block copolymer composition (i.e. same
24 target DP of PHPMA) at different total solids concentration ranging from 10-20 wt%,
25 comparable *M*_{*n*} values were measured throughout. Low dispersity values were calculated
26
27
28
29
30
31
32
33
34
35
36
37
38
39
40
41
42
43
44
45
46
47
48
49
50
51
52
53
54
55
56
57
58
59
60

1
2
3 when targeting shorter PHPMA blocks with increasing D_M upon gradually increasing either
4 the DP of the core-forming block or the total solids content (Figure 2D and Table S1). This
5 behavior of M_n and D_M values' progression is typical for dispersion PISA systems.
6
7

8
9
10 Exhaustive dry-state stained transmission electron microscopy (TEM) imaging along with
11 dynamic light scattering (DLS) and zeta-potential analyses were used for the characterization
12 of PSar₅₉-*b*-PHPMA_n block copolymer nano-objects in solution (Figures S7-S18 and Table
13 S2, SI). Morphologies evolving from spherical micelles (S - spheres) to worm-like micelles
14 (W - worms) and vesicular nanostructures (V - vesicles) along with intermediate mixed
15 morphologies were observed upon targeting higher DPs of the core-forming PHPMA block
16 and solids concentration. In particular, a mixture of spheres and short worms was obtained in
17 the case of PSar₅₉-*b*-PHPMA₁₀₀ diblock copolymer system at [solids] = 10 and 15 wt%, while
18 a pure phase of worms could be accessed for the same block copolymer composition at 20
19 wt%, as sphere-sphere fusion is more favorable at higher solids content. This was evident
20 macroscopically by the formation of a clear free-standing gel in the reaction vial after photo-
21 PISA. In all three cases, low hydrodynamic diameter (D_h) and polydispersity (PD) values were
22 measured ranging from 29 - 47 nm and 0.06 - 0.16, respectively, accompanied by narrow
23 particle size distributions. Aqueous photo-PISA reaction targeting $DP_{\text{PHPMA}} = 200$ at [solids]
24 = 10 wt% lead to the formation of a mixed phase of all three morphologies (S+W+V), due to
25 coexistence of two particle populations initially indicated by DLS analysis and shown by
26 TEM imaging. A mixture of worm-like micelles and spherical vesicles was formed for the
27 same DP of PHPMA at [solids] = 15 and 20 wt%. In these cases D_h and PD values were found
28 to be relatively higher ($D_h = 200 - 500$ nm and PD = 0.13 - 0.36) compared to the ones
29 corresponding to PSar₅₉-*b*-PHPMA₁₀₀ due to existence of mixed morphologies of small and
30
31
32
33
34
35
36
37
38
39
40
41
42
43
44
45
46
47
48
49
50
51
52
53
54
55
56
57
58
59
60

1
2
3 larger nano-objects. For $DP_{\text{PHPMA}} = 300$ at $[\text{solids}] = 10 \text{ wt}\%$, an intermediate morphology
4
5 between worms and vesicles was observed, while pure vesicular morphologies were formed
6
7 at higher solids concentrations for the same target DP of PHPMA. Interestingly, a pure phase
8
9 of long tubular vesicles was detected for $\text{PSar}_{59}\text{-}b\text{-PHPMA}_{300}$ at $[\text{solids}] = 15 \text{ wt}\%$ of average
10
11 $D_h = 1360 \text{ nm}$ and $PD = 0.22$ showing great promise for nanocarrier design applications as it
12
13 is proven that non-spherical particles exhibit longer circulation times *in vivo* and could be
14
15 more easily uptaken by cells.⁶⁴ In the case of 20 wt% total solids content for $DP_{\text{PHPMA}} = 300$,
16
17 micron-sized oligolamellar vesicles of relatively low PD were detected by dry-state TEM
18
19 imaging. More importantly, pure spherical and elongated unilamellar vesicles with $D_h = 321$
20
21 nm and narrow particles' size distribution were obtained for $\text{PSar}_{59}\text{-}b\text{-PHPMA}_{400}$ formed at
22
23 10 wt% that could potentially be utilized for nanoreactor development. Finally, a mixture of
24
25 elongated tubular and multilamellar vesicles was formed in case of $DP_{\text{PHPMA}} = 400$ at $[\text{solids}]$
26
27 = 15 wt%, while an intriguing morphology of large perforated vesicles with $D_h = 1515 \text{ nm}$
28
29 and $PD = 0.22$ was observed at 20 wt% solids content. The unusual higher-order vesicular
30
31 morphologies observed at exceedingly high DPs and wt% of PHPMA are mainly attributed
32
33 to the development of significant hydrophobic interactions between the PHPMA cores and
34
35 the short hydrophobic segment of hexylamine located in front of the hydrophilic stabilizer
36
37 block of PSar that could promote further entanglement of the polymer chains and formation
38
39 of loops potentially aiding the fabrication of flower-like nanostructures.

40
41
42 Based on the obtained results, a detailed phase diagram was constructed to summarize the
43
44 observed nano-object morphologies of different $\text{PSar}_{59}\text{-}b\text{-PHPMA}_n$ formulations developed
45
46 upon varying DP_{PHPMA} and $[\text{solids}]$ (wt%) and to allow for the facile reproducibility of our
47
48 findings (Figure 3). Importantly, in all $\text{PSar}_{59}\text{-}b\text{-PHPMA}_n$ nano-object formulations, zeta-

potential values of around 0 mV (zeta-potential = $-0.15 - +0.07$ mV) were measured from microelectrophoretic analysis at neutral pH that were independent of pH variations from acidic (pH = 4.0) to basic (pH = 9.0) values (Table S2, SI), revealing the absence of net charges on the outer surface of particles and their promising “stealth” character as they can prevent the activation of the immune system upon insertion to the body.

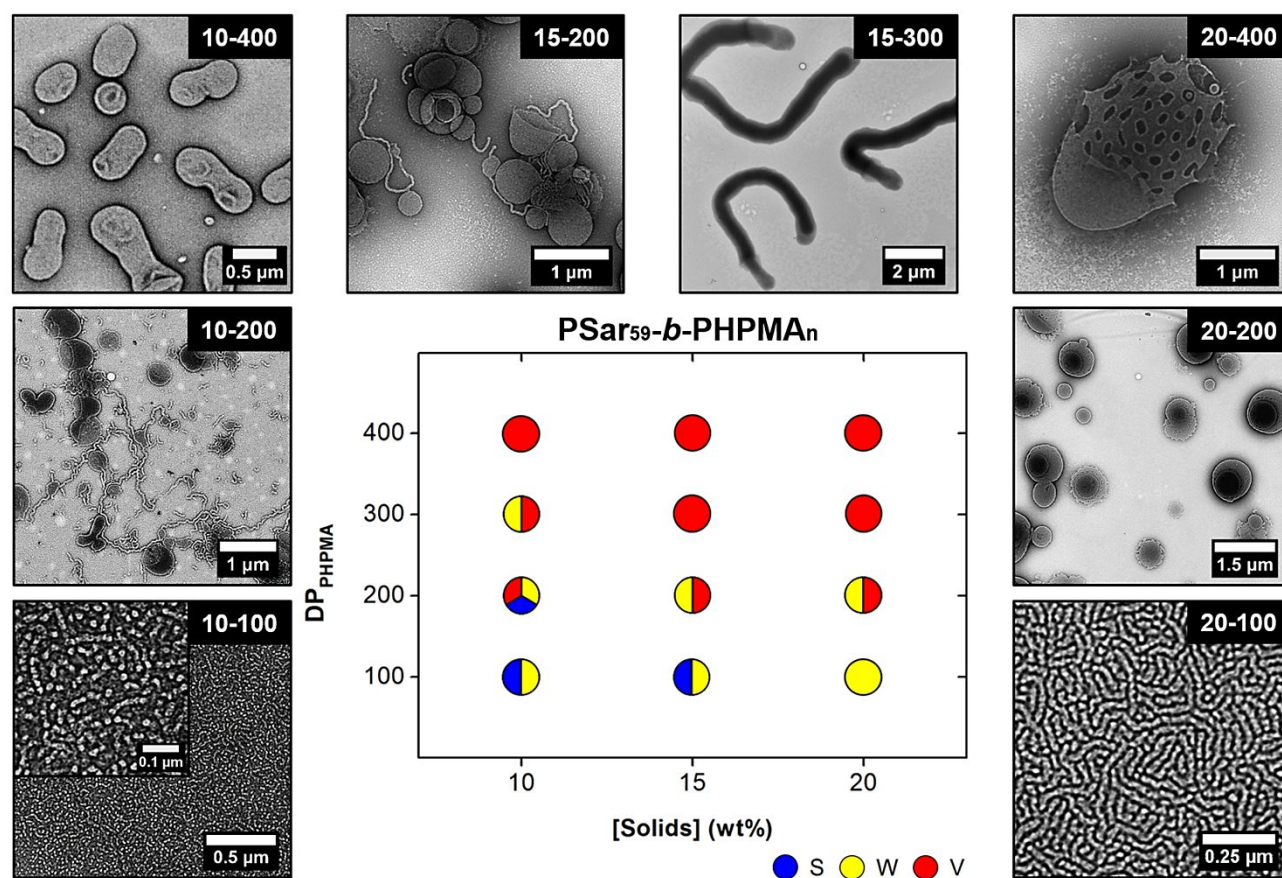


Figure 3. Detailed morphologies diagram for $PSar_{59}-b-PHPMA_n$ diblock copolymer nano-objects prepared *via* aqueous RAFT-mediated photo-PISA of HPMA by varying the total solids content and DP of PHPMA, along with representative dry-state TEM images of different formulations, stained with 1 wt% uranyl acetate (UA) solution. Key: S – spherical micelles (blue), W – worm-like micelles (yellow), V – vesicles (red).

1
2
3 **Colloidal stability of PSar₅₉-*b*-PHPMA₄₀₀ unilamellar vesicles and resistance against**
4 **degradation by proteolytic enzymes.** Based on the constructed morphologies diagram, the

5
6 developed PSar₅₉-*b*-PHPMA₄₀₀ unilamellar vesicles formed at 10 wt% solids as a pure
7 morphology were isolated and their potential use for nanoreactor fabrication and future *in*
8 *vitro* and *in vivo* studies was explored. Additionally, the resistance of both empty and enzyme-
9 loaded vesicles against a series of different proteases was also assessed.

10
11 First, the colloidal stability of empty PSar₅₉-*b*-PHPMA₄₀₀ vesicles in a range of complex
12 media (i.e. DI water, fetal bovine serum (FBS) and cell culture medium) was evaluated, by
13 monitoring the D_h changes over time using DLS upon incubation at 37 °C for a total time
14 period of 72 h (Figure S19, SI). Not surprisingly, the average size of vesicles in DI water
15 didn't change significantly over extended incubation periods ranging from 340 to 380 nm. In
16 the case of vesicles incubated in aqueous FBS solution, a negligible D_h increase to 405 nm
17 was observed after 24 h of incubation time which was more evident after 72 h ($D_h = 448$ nm),
18 indicating slow time-dependent agglomeration of particles with blood components such as
19 serum proteins (e.g. albumins and globulins).⁶² On the contrary, for empty vesicles incubated
20 in cell growth medium, a minor D_h decrease was observed after 24 h of incubation time to
21 220 nm while their size remained constant for the rest of the study. Overall, the obtained
22 results revealed the good colloidal properties of PSar₅₉-*b*-PHPMA₄₀₀ vesicles in physiological
23 media for prolonged time periods.

24
25 Additionally, to further assess the effect of common proteolytic enzymes on the PSar
26 poly(peptoid) corona of PSar₅₉-*b*-PHPMA₄₀₀ vesicles and the potential ability of the formed
27 nanostructures to act as protective cages of delicate enzymes for development of vesicular
28 nanoreactors, particle solutions at 10-fold dilution from original concentration were incubated
29
30
31
32
33
34
35
36
37
38
39
40
41
42
43
44
45
46
47
48
49
50
51
52
53
54
55
56
57
58
59
60

1
2
3 with a series of proteases (i.e. α -chymotrypsin, trypsin and pepsin) at 37 °C and appropriate
4 pH for a period of 72 h (Figure 4). Structural and molecular characteristics' changes of empty
5
6 PSar₅₉-*b*-PHPMA₄₀₀ were monitored by DLS and SEC analyses and dry-state TEM imaging
7
8 for determination of the ability of hydrophilic and non-ionic PSar₅₉ stabilizer block to resist
9
10 proteolysis. Size variations of the vesicle solutions incubated with either α -chymotrypsin (α -
11
12 CT) or trypsin at pH = 7.0 and pepsin at pH = 1.8 were measured by DLS analysis (Figure
13
14 4A). In case of α -CT and trypsin, the overall dimensions of particles remained constant in the
15
16 range of 305-335 nm for the total incubation period of 72 h, while for pepsin a slight size
17
18 increase to 380 nm was monitored after 24 h mainly attributed to the exceedingly low pH
19
20 level of the solution affecting the measurements upon extended incubation time periods. Near-
21
22 identical SEC molecular weight distributions were recorded for lyophilized samples in all
23
24 three cases with M_n and D_M values being similar to those of empty PSar₅₉-*b*-PHPMA₄₀₀
25
26 diblock copolymers formed by aqueous photo-PISA at 10 wt% (Figure 4B), showing no
27
28 apparent peptoid bond hydrolysis taking place. Dry-state TEM imaging of empty vesicles
29
30 after 72 h of incubation time with each protease proved that no changes in shape and size of
31
32 nano-objects occurred showing their excellent stability toward biodegradation from various
33
34 proteolytic enzymes (Figures 4C and S20, SI).

35
36
37
38
39
40
41
42 Based on these findings, the ability of PSar₅₉-*b*-PHPMA₄₀₀ vesicles to protect other sensitive
43
44 hydrophilic enzymes from proteolysis by encapsulation in their inner aqueous lumen compared to
45
46 free enzymes was further investigated. Horseradish peroxidase (HRP) was selected as a model
47
48 enzyme for encapsulation into PSar₅₉-*b*-PHPMA₄₀₀ vesicles *via* a one-pot photo-PISA
49
50 methodology previously described by our group.⁵⁷⁻⁵⁹ In these studies, it was shown that such
51
52 enzymes could tolerate photo-PISA reaction conditions, retain activity and communicate with the
53
54
55
56
57
58
59
60

1
2
3 external aqueous environment by passive diffusion of small molecules through the semipermeable
4 and relatively hydrated PHPMA membrane of vesicles providing a read-out of permeability.
5
6 Indeed, control experiments of either purging a HRP solution with N₂ (g) for 15 min or exposure
7
8 to 405 nm irradiation for 90 min after N₂ (g) bubbling showed no loss of enzyme activity as
9
10 compared to the untreated enzyme (Figure S21, SI). Purified HRP-loaded vesicular nanoreactors
11
12 and free HRP were incubated with either a-CT or trypsin at pH = 7.0 for 72 h, and their relative
13
14 activities were determined by colorimetric assays at $\lambda = 492$ nm over time and were normalized
15
16 against control experiments of HRP-loaded vesicles and free enzyme incubated solely with
17
18 phosphate buffer at pH = 7.0 in absence of proteases. It should be noted that pepsin was not used
19
20 for incubation of HRP-loaded vesicles as the optimum pH ranges of the two enzymes differ
21
22 significantly. As shown in Figure 4D, quantitative retention of activity was achieved in case of
23
24 HRP-loaded vesicles after 18 and 72 h of incubation time with either a-CT (96%) or trypsin (92%).
25
26 On the contrary, a significant loss of activity of 29.2% for a-CT and 41% for trypsin was noticed
27
28 in case of free HRP attributed to gradual enzyme degradation from the different proteases after 18
29
30 h. An additional activity decrease to 54.9% for a-CT and 32.9% for trypsin was measured for the
31
32 free enzyme solution after 72 h, clearly showing the robust nature and protective character of PSar-
33
34 based vesicles toward other encapsulated biomolecules.
35
36
37
38
39
40
41

42 Importantly, when performing the described studies to determine the resistance against proteolytic
43
44 degradation of purified empty and HRP-loaded PEG₁₁₃-*b*-PHPMA₄₀₀ unilamellar vesicles of
45
46 similar size and overall characteristics previously developed by our group,⁴² a near-identical
47
48 retention of enzyme activity was observed in the case of HRP-loaded vesicles after 18 and 72 h of
49
50 incubation time with either a-CT or trypsin. However, a significant D_h and PD increase was
51
52 monitored in the case of empty PEG₁₁₃-*b*-PHPMA₄₀₀ unilamellar vesicles after 18 h of incubation
53
54
55
56
57
58
59
60

time with different proteases (a-CT, trypsin or pepsin), as judged by DLS analysis, mainly attributed to the enhanced protein-induced particle aggregation that occurs in this case after a certain incubation period (Figure S22, SI).

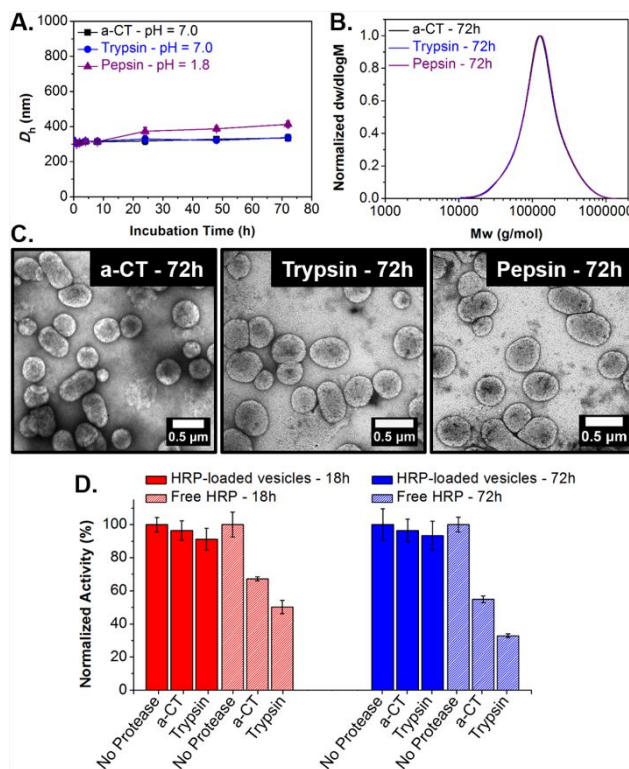


Figure 4. (A) Monitoring of hydrodynamic diameter (D_h) changes of empty PSAr₅₉-b-PHPMA₄₀₀ vesicles in 100 mM PB upon incubation with a-CT (pH = 7.0), trypsin (pH = 7.0) or pepsin (pH = 1.8) at 37 °C for 72 h (the error bars show the standard deviation from five repeat measurements). (B) Normalized SEC RI molecular weight distributions for PSAr₅₉-b-PHPMA_n diblock copolymers after incubation with a-CT (pH = 7.0), trypsin (pH = 7.0) or pepsin (pH = 1.8) at 37 °C for 72 h. M_n and D_M values were calculated from PMMA standards using 5 mM NH₄BF₄ in DMF as the eluent. (C) Representative dry-state TEM images of empty PSAr₅₉-b-PHPMA₄₀₀ vesicles after incubation with a-CT (pH = 7.0), trypsin (pH = 7.0) or pepsin (pH = 1.8) for 72 h, stained with 1 wt% UA. (D) Normalized relative activities of HRP-loaded PSAr₅₉-b-PHPMA₄₀₀ vesicles and free HRP after incubation with a-CT or trypsin at 37 °C for 18 h (red) and 72 h (blue) (the error shows the standard deviation from four repeat measurements). The normalized relative activities are defined as the ratio between the

1
2
3 absorbance of the samples and the absorbance of untreated HRP-loaded vesicles or free HRP,
4 respectively, at the end point of the enzymatic assay (end point = 30 min, $\lambda = 492$ nm).
5
6
7
8
9

10 CONCLUSIONS

11
12
13 To conclude, we demonstrate an efficient methodology for the fabrication of poly(peptoid)-
14 based block copolymer nano-objects with predictable morphologies at high concentrations
15 by combining living NCA ROP and aqueous RAFT-mediated photo-PISA. In particular,
16 poly(sarcosine) was utilized as a novel hydrophilic stabilizer block for controlled RAFT
17 chain-extensions of a methacrylate monomer able to undergo PISA under aqueous
18 dispersion polymerization conditions targeting different DPs of the core-forming block and
19 total solids concentrations. A diverse set of nano-object morphologies including higher-
20 order structures was obtained, as evidenced by the construction of a phase diagram. The
21 colloidal stability of single phase vesicles and their ability to encapsulate hydrophilic
22 enzymes protecting them from proteolysis were thoroughly assessed and compared to their
23 PEG-based counterparts, showing great promise for use of the developed materials in
24 various biomedical applications. Our findings circumvent the current limitations of
25 conventional block copolymer self-assembly techniques, such as dilute conditions and
26 multiple laborious post-polymerization processing and purification steps for targeting
27 certain morphologies, underlining the potential of poly(sarcosine) as an alternative corona-
28 forming polymer to PEG-derived polymers for fabrication of PISA nano-objects with bio-
29 relevant character.
30
31
32
33
34
35
36
37
38
39
40
41
42
43
44
45
46
47
48
49
50
51
52
53
54
55
56
57
58
59
60

1
2
3 ASSOCIATED CONTENT
4
5

6 **Supporting Information**
7

8
9 The Supporting Information is available free of charge on the ACS Publications website at DOI:
10
11 10.1021/acs.bio-mac.xbxxxxx.
12
13

14
15 Materials and characterization methods, additional NMR, FT-IR, SEC and DLS data,
16
17 additional dry-state TEM images, HRP control experiments and colloidal stability results.
18
19

20 AUTHOR INFORMATION
21

22
23 **Corresponding Authors**
24

25
26 *Email: nikolaos.hadjichristidis@kaust.edu.sa
27

28 *Email: r.oreilly@bham.ac.uk
29
30

31 **Author Contributions**
32

33
34 The manuscript was written through contributions of all authors. All authors have given approval
35
36 to the final version of the manuscript.
37
38

39 **Notes**
40

41 The authors declare no competing financial interest.
42
43
44

45 ACKNOWLEDGEMENTS
46

47
48 This work was supported by the ERC (grant number 615142), EPSRC and King Abdullah
49
50 University of Science and Technology (KAUST).
51
52
53

54 REFERENCES
55
56
57
58
59
60

1. Knop, K.; Hoogenboom, R.; Fischer, D.; Schubert, U. S., Poly(ethylene glycol) in Drug Delivery: Pros and Cons as Well as Potential Alternatives. *Angew. Chem. Int. Ed.* **2010**, *49*, (36), 6288-6308.
2. Jokerst, J. V.; Lobovkina, T.; Zare, R. N.; Gambhir, S. S., Nanoparticle PEGylation for imaging and therapy. *Nanomedicine* **2011**, *6*, (4), 715-728.
3. Cui, S.; Pan, X.; Gebru, H.; Wang, X.; Liu, J.; Liu, J.; Li, Z.; Guo, K., Amphiphilic star-shaped poly(sarcosine)-block-poly(ϵ -caprolactone) diblock copolymers: one-pot synthesis, characterization, and solution properties. *J. Mater. Chem. B* **2017**, *5*, (4), 679-690.
4. Veronese, F. M.; Pasut, G., PEGylation, successful approach to drug delivery. *Drug Discov. Today* **2005**, *10*, (21), 1451-1458.
5. Turecek, P. L.; Bossard, M. J.; Schoetens, F.; Ivens, I. A., PEGylation of Biopharmaceuticals: A Review of Chemistry and Nonclinical Safety Information of Approved Drugs. *J. Pharm. Sci.* **2016**, *105*, (2), 460-475.
6. Jo, S.; Park, K., Surface modification using silanated poly(ethylene glycol)s. *Biomaterials* **2000**, *21*, (6), 605-616.
7. Fruijtier-Pölloth, C., Safety assessment on polyethylene glycols (PEGs) and their derivatives as used in cosmetic products. *Toxicology* **2005**, *214*, (1), 1-38.
8. Wang, Z.; Song, J.; Zhang, S.; Xu, X.-Q.; Wang, Y., Formulating Polyethylene Glycol as Supramolecular Emulsifiers for One-Step Double Emulsions. *Langmuir* **2017**, *33*, (36), 9160-9169.
9. Lee, Y.-A.; Kim, Y.-H.; Kim, B.-J.; Jung, M.-S.; Auh, J.-H.; Seo, J.-T.; Park, Y.-S.; Lee, S.-H.; Ryu, B.-Y., Cryopreservation of Mouse Spermatogonial Stem Cells in Dimethylsulfoxide and Polyethylene Glycol1. *Biol. Reprod.* **2013**, *89*, (5), 109, 1-9.
10. Harris, J. M.; Chess, R. B., Effect of pegylation on pharmaceuticals. *Nat. Rev. Drug Discovery* **2003**, *2*, 214-221.
11. Ishida, T.; Harada, M.; Wang, X. Y.; Ichihara, M.; Irimura, K.; Kiwada, H., Accelerated blood clearance of PEGylated liposomes following preceding liposome injection: Effects of lipid dose and PEG surface-density and chain length of the first-dose liposomes. *J. Controlled Release* **2005**, *105*, (3), 305-317.
12. Garay, R. P.; El-Gewely, R.; Armstrong, J. K.; Garratty, G.; Richette, P., Antibodies against polyethylene glycol in healthy subjects and in patients treated with PEG-conjugated agents. *Expert Opin. Drug Deliv.* **2012**, *9*, (11), 1319-1323.
13. Deng, Y.; Zou, T.; Tao, X.; Semetey, V.; Trepout, S.; Marco, S.; Ling, J.; Li, M.-H., Poly(ϵ -caprolactone)-block-polysarcosine by Ring-Opening Polymerization of Sarcosine N-Thiocarboxyanhydride: Synthesis and Thermoresponsive Self-Assembly. *Biomacromolecules* **2015**, *16*, (10), 3265-3274.
14. Hu, Y.; Hou, Y.; Wang, H.; Lu, H., Polysarcosine as an Alternative to PEG for Therapeutic Protein Conjugation. *Bioconjugate Chem.* **2018**, *29*, (7), 2232-2238.
15. Pelegri-O'Day, E. M.; Lin, E.-W.; Maynard, H. D., Therapeutic Protein-Polymer Conjugates: Advancing Beyond PEGylation. *J. Am. Chem. Soc.* **2014**, *136*, (41), 14323-14332.
16. Zhang, H.; Grinstaff, M. W., Recent Advances in Glycerol Polymers: Chemistry and Biomedical Applications. *Macromol. Rapid Commun.* **2014**, *35*, (22), 1906-1924.
17. Hoogenboom, R., Poly(2-oxazoline)s: A Polymer Class with Numerous Potential Applications. *Angew. Chem. Int. Ed.* **2009**, *48*, (43), 7978-7994.
18. Liarou, E.; Varlas, S.; Skoulas, D.; Tsimblouli, C.; Sereti, E.; Dimas, K.; Iatrou, H., Smart polymersomes and hydrogels from polypeptide-based polymer systems through α -amino acid N-

1
2
3 carboxyanhydride ring-opening polymerization. From chemistry to biomedical applications. *Prog.*
4 *Polym. Sci.* **2018**, 83, 28-78.

5 19. Secker, C.; Brosnan, S. M.; Luxenhofer, R.; Schlaad, H., Poly(α -Peptoids) Revisited:
6 Synthesis, Properties, and Use as Biomaterial. *Macromol. Biosci.* **2015**, 15, (7), 881-891.

7 20. Gangloff, N.; Ulbricht, J.; Lorson, T.; Schlaad, H.; Luxenhofer, R., Peptoids and
8 Polypeptoids at the Frontier of Supra- and Macromolecular Engineering. *Chem. Rev.* **2016**, 116,
9 (4), 1753-1802.

10 21. Mudd, S. H.; Ebert, M. H.; Scriver, C. R., Labile methyl group balances in the human: The
11 role of sarcosine. *Metabolism* **1980**, 29, (8), 707-720.

12 22. Weber, B.; Seidl, C.; Schwiertz, D.; Scherer, M.; Bleher, S.; Süß, R.; Barz, M.,
13 Polysarcosine-Based Lipids: From Lipopolypeptoid Micelles to Stealth-Like Lipids in Langmuir
14 Blodgett Monolayers. *Polymers* **2016**, 8, (12), 427.

15 23. Birke, A.; Ling, J.; Barz, M., Polysarcosine-containing copolymers: Synthesis,
16 characterization, self-assembly, and applications. *Prog. Polym. Sci.* **2018**, 81, 163-208.

17 24. Fokina, A.; Klinker, K.; Braun, L.; Jeong, B. G.; Bae, W. K.; Barz, M.; Zentel, R.,
18 Multidentate Polysarcosine-Based Ligands for Water-Soluble Quantum Dots. *Macromolecules*
19 **2016**, 49, (10), 3663-3671.

20 25. Hadjichristidis, N.; Iatrou, H.; Pitsikalis, M.; Sakellariou, G., Synthesis of Well-Defined
21 Polypeptide-Based Materials via the Ring-Opening Polymerization of α -Amino Acid N-
22 Carboxyanhydrides. *Chem. Rev.* **2009**, 109, (11), 5528-5578.

23 26. Zhang, D.; Lahasky, S. H.; Guo, L.; Lee, C.-U.; Lavan, M., Polypeptoid Materials: Current
24 Status and Future Perspectives. *Macromolecules* **2012**, 45, (15), 5833-5841.

25 27. Birke, A.; Huesmann, D.; Kelsch, A.; Weilbacher, M.; Xie, J.; Bros, M.; Bopp, T.; Becker,
26 C.; Landfester, K.; Barz, M., Polypeptoid-block-polypeptide Copolymers: Synthesis,
27 Characterization, and Application of Amphiphilic Block Copolypept(o)ides in Drug Formulations
28 and Miniemulsion Techniques. *Biomacromolecules* **2014**, 15, (2), 548-557.

29 28. Huesmann, D.; Sevenich, A.; Weber, B.; Barz, M., A head-to-head comparison of
30 poly(sarcosine) and poly(ethylene glycol) in peptidic, amphiphilic block copolymers. *Polymer*
31 **2015**, 67, 240-248.

32 29. Fetsch, C.; Gaitzsch, J.; Messenger, L.; Battaglia, G.; Luxenhofer, R., Self-Assembly of
33 Amphiphilic Block Copolypeptoids – Micelles, Worms and Polymersomes. *Sci. Rep.* **2016**, 6,
34 33491.

35 30. Weber, B.; Kappel, C.; Scherer, M.; Helm, M.; Bros, M.; Grabbe, S.; Barz, M., PeptoSomes
36 for Vaccination: Combining Antigen and Adjuvant in Polypept(o)ide-Based Polymersomes.
37 *Macromol. Biosci.* **2017**, 17, (10), 1700061.

38 31. Makino, A.; Hara, E.; Hara, I.; Ozeki, E.; Kimura, S., Size Control of Core-Shell-type
39 Polymeric Micelle with a Nanometer Precision. *Langmuir* **2014**, 30, (2), 669-674.

40 32. Kim, C. J.; Ueda, M.; Imai, T.; Sugiyama, J.; Kimura, S., Tuning the Viscoelasticity of
41 Peptide Vesicles by Adjusting Hydrophobic Helical Blocks Comprising Amphiphilic
42 Polypeptides. *Langmuir* **2017**, 33, (22), 5423-5429.

43 33. Warren, N. J.; Mykhaylyk, O. O.; Mahmood, D.; Ryan, A. J.; Armes, S. P., RAFT aqueous
44 dispersion polymerization yields poly(ethylene glycol)-based diblock copolymer nano-objects
45 with predictable single phase morphologies. *J. Am. Chem. Soc.* **2014**, 136, (3), 1023-33.

46 34. Warren, N. J.; Armes, S. P., Polymerization-induced self-assembly of block copolymer
47 nano-objects via RAFT aqueous dispersion polymerization. *J. Am. Chem. Soc.* **2014**, 136, (29),
48 10174-85.

- 1
2
3 35. Canning, S. L.; Smith, G. N.; Armes, S. P., A Critical Appraisal of RAFT-Mediated
4 Polymerization-Induced Self-Assembly. *Macromolecules* **2016**, 49, (6), 1985-2001.
- 5 36. Derry, M. J.; Fielding, L. A.; Armes, S. P., Polymerization-induced self-assembly of block
6 copolymer nanoparticles via RAFT non-aqueous dispersion polymerization. *Prog. Polym. Sci.*
7 **2016**, 52, 1-18.
- 8 37. Wang, G.; Schmitt, M.; Wang, Z.; Lee, B.; Pan, X.; Fu, L.; Yan, J.; Li, S.; Xie, G.;
9 Bockstaller, M. R.; Matyjaszewski, K., Polymerization-Induced Self-Assembly (PISA) Using
10 ICAR ATRP at Low Catalyst Concentration. *Macromolecules* **2016**, 49, (22), 8605-8615.
- 11 38. Obeng, M.; Milani, A. H.; Musa, M. S.; Cui, Z.; Fielding, L. A.; Farrand, L.; Goulding,
12 M.; Saunders, B. R., Self-assembly of poly(lauryl methacrylate)-b-poly(benzyl methacrylate)
13 nano-objects synthesised by ATRP and their temperature-responsive dispersion properties. *Soft*
14 *Matter* **2017**, 13, (11), 2228-2238.
- 15 39. Qiao, X. G.; Lansalot, M.; Bourgeat-Lami, E.; Charleux, B., Nitroxide-Mediated
16 Polymerization-Induced Self-Assembly of Poly(poly(ethylene oxide) methyl ether methacrylate-
17 co-styrene)-b-poly(n-butyl methacrylate-co-styrene) Amphiphilic Block Copolymers.
18 *Macromolecules* **2013**, 46, (11), 4285-4295.
- 19 40. Qiao, X. G.; Dugas, P. Y.; Charleux, B.; Lansalot, M.; Bourgeat-Lami, E., Nitroxide-
20 mediated polymerization-induced self-assembly of amphiphilic block copolymers with a
21 pH/temperature dual sensitive stabilizer block. *Polym. Chem.* **2017**, 8, (27), 4014-4029.
- 22 41. Williams, M.; Penfold, N. J. W.; Lovett, J. R.; Warren, N. J.; Douglas, C. W. I.;
23 Doroshenko, N.; Verstraete, P.; Smets, J.; Armes, S. P., Bespoke cationic nano-objects via RAFT
24 aqueous dispersion polymerisation. *Polym. Chem.* **2016**, 7, (23), 3864-3873.
- 25 42. Blackman, L. D.; Doncom, K. E. B.; Gibson, M. I.; O'Reilly, R. K., Comparison of photo-
26 and thermally initiated polymerization-induced self-assembly: a lack of end group fidelity drives
27 the formation of higher order morphologies. *Polym. Chem.* **2017**, 8, (18), 2860-2871.
- 28 43. Deng, R.; Derry, M. J.; Mable, C. J.; Ning, Y.; Armes, S. P., Using Dynamic Covalent
29 Chemistry To Drive Morphological Transitions: Controlled Release of Encapsulated
30 Nanoparticles from Block Copolymer Vesicles. *J. Am. Chem. Soc.* **2017**, 139, (22), 7616-7623.
- 31 44. Khor, S. Y.; Truong, N. P.; Quinn, J. F.; Whittaker, M. R.; Davis, T. P., Polymerization-
32 Induced Self-Assembly: The Effect of End Group and Initiator Concentration on Morphology of
33 Nanoparticles Prepared via RAFT Aqueous Emulsion Polymerization. *ACS Macro Lett.* **2017**, 6,
34 (9), 1013-1019.
- 35 45. Wright, D. B.; Touve, M. A.; Thompson, M. P.; Gianneschi, N. C., Aqueous-Phase Ring-
36 Opening Metathesis Polymerization-Induced Self-Assembly. *ACS Macro Lett.* **2018**, 7, (4), 401-
37 405.
- 38 46. Foster, J. C.; Varlas, S.; Blackman, L. D.; Arkinstall, L. A.; O'Reilly, R. K., Ring-Opening
39 Metathesis Polymerization in Aqueous Media Using a Macroinitiator Approach. *Angew. Chem.*
40 *Int. Ed.* **2018**, 57, (33), 10672-10676.
- 41 47. Wright, D. B.; Touve, M. A.; Adamiak, L.; Gianneschi, N. C., ROMPISA: Ring-Opening
42 Metathesis Polymerization-Induced Self-Assembly. *ACS Macro Lett.* **2017**, 6, (9), 925-929.
- 43 48. Tan, J.; Sun, H.; Yu, M.; Sumerlin, B. S.; Zhang, L., Photo-PISA: Shedding Light on
44 Polymerization-Induced Self-Assembly. *ACS Macro Lett.* **2015**, 4, (11), 1249-1253.
- 45 49. Yeow, J.; Xu, J.; Boyer, C., Polymerization-Induced Self-Assembly Using Visible Light
46 Mediated Photoinduced Electron Transfer-Reversible Addition-Fragmentation Chain Transfer
47 Polymerization. *ACS Macro Lett.* **2015**, 4, (9), 984-990.
- 48
49
50
51
52
53
54
55
56
57
58
59
60

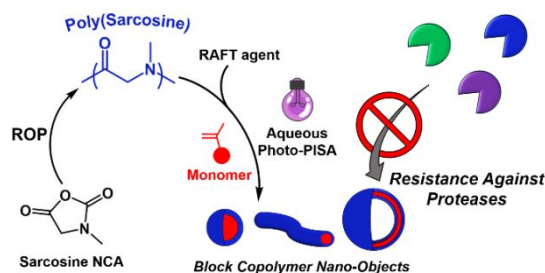
- 1
2
3 50. Tan, J.; Bai, Y.; Zhang, X.; Zhang, L., Room temperature synthesis of poly(poly(ethylene
4 glycol) methyl ether methacrylate)-based diblock copolymer nano-objects via Photoinitiated
5 Polymerization-Induced Self-Assembly (Photo-PISA). *Polym. Chem.* **2016**, *7*, (13), 2372-2380.
- 6 51. Ng, G.; Yeow, J.; Xu, J.; Boyer, C., Application of oxygen tolerant PET-RAFT to
7 polymerization-induced self-assembly. *Polym. Chem.* **2017**, *8*, (18), 2841-2851.
- 8 52. Tan, J.; Liu, D.; Bai, Y.; Huang, C.; Li, X.; He, J.; Xu, Q.; Zhang, X.; Zhang, L., An insight
9 into aqueous photoinitiated polymerization-induced self-assembly (photo-PISA) for the
10 preparation of diblock copolymer nano-objects. *Polym. Chem.* **2017**, *8*, (8), 1315-1327.
- 11 53. Yeow, J.; Boyer, C., Photoinitiated Polymerization-Induced Self-Assembly (Photo-PISA):
12 New Insights and Opportunities. *Adv. Sci.* **2017**, *4*, (7), 1700137.
- 13 54. Burrige, K. M.; Wright, T. A.; Page, R. C.; Konkolewicz, D., Photochemistry for Well-
14 Defined Polymers in Aqueous Media: From Fundamentals to Polymer Nanoparticles to
15 Bioconjugates. *Macromol. Rapid Commun.* **2018**, *39*, (12), 1800093.
- 16 55. Tan, J.; Zhang, X.; Liu, D.; Bai, Y.; Huang, C.; Li, X.; Zhang, L., Facile Preparation of
17 CO₂-Responsive Polymer Nano-Objects via Aqueous Photoinitiated Polymerization-Induced
18 Self-Assembly (Photo-PISA). *Macromol. Rapid Commun.* **2016**, *38*, (13), 1600508.
- 19 56. Tan, J.; Liu, D.; Bai, Y.; Huang, C.; Li, X.; He, J.; Xu, Q.; Zhang, L., Enzyme-Assisted
20 Photoinitiated Polymerization-Induced Self-Assembly: An Oxygen-Tolerant Method for
21 Preparing Block Copolymer Nano-Objects in Open Vessels and Multiwell Plates. *Macromolecules*
22 **2017**, *50*, (15), 5798-5806.
- 23 57. Blackman, L. D.; Varlas, S.; Arno, M. C.; Fayter, A.; Gibson, M. I.; O'Reilly, R. K.,
24 Permeable Protein-Loaded Polymersome Cascade Nanoreactors by Polymerization-Induced Self-
25 Assembly. *ACS Macro Lett.* **2017**, *6*, (11), 1263-1267.
- 26 58. Blackman, L. D.; Varlas, S.; Arno, M. C.; Houston, Z. H.; Fletcher, N. L.; Thurecht, K. J.;
27 Hasan, M.; Gibson, M. I.; O'Reilly, R. K., Confinement of Therapeutic Enzymes in Selectively
28 Permeable Polymer Vesicles by Polymerization-Induced Self-Assembly (PISA) Reduces
29 Antibody Binding and Proteolytic Susceptibility. *ACS Cent. Sci.* **2018**, *4*, (6), 718-723.
- 30 59. Varlas, S.; Blackman, L. D.; Findlay, H. E.; Reading, E.; Booth, P. J.; Gibson, M. I.;
31 O'Reilly, R. K., Photoinitiated Polymerization-Induced Self-Assembly in the Presence of
32 Surfactants Enables Membrane Protein Incorporation into Vesicles. *Macromolecules* **2018**, *51*,
33 (6), 6190-6201.
- 34 60. Weber, B.; Birke, A.; Fischer, K.; Schmidt, M.; Barz, M., Solution Properties of
35 Polysarcosine: From Absolute and Relative Molar Mass Determinations to Complement
36 Activation. *Macromolecules* **2018**, *51*, (7), 2653-2661.
- 37 61. Johnson, R. N.; Burke, R. S.; Convertine, A. J.; Hoffman, A. S.; Stayton, P. S.; Pun, S. H.,
38 Synthesis of Statistical Copolymers Containing Multiple Functional Peptides for Nucleic Acid
39 Delivery. *Biomacromolecules* **2010**, *11*, (11), 3007-3013.
- 40 62. Bilalis, P.; Tziveleka, L.-A.; Varlas, S.; Iatrou, H., pH-Sensitive nanogates based on poly(l-
41 histidine) for controlled drug release from mesoporous silica nanoparticles. *Polym. Chem.* **2016**,
42 *7*, (7), 1475-1485.
- 43 63. Tan, J.; He, J.; Li, X.; Xu, Q.; Huang, C.; Liu, D.; Zhang, L., Rapid synthesis of well-
44 defined all-acrylic diblock copolymer nano-objects via alcoholic photoinitiated polymerization-
45 induced self-assembly (photo-PISA). *Polym. Chem.* **2017**, *8*, (44), 6853-6864.
- 46 64. Robertson, J. D.; Yealland, G.; Avila-Olias, M.; Chierico, L.; Bandmann, O.; Renshaw, S.
47 A.; Battaglia, G., pH-Sensitive Tubular Polymersomes: Formation and Applications in Cellular
48 Delivery. *ACS Nano* **2014**, *8*, (5), 4650-4661.
- 49
50
51
52
53
54
55
56
57
58
59
60

1
2
3
4
5
6
7
8
9
10
11
12
13
14
15
16
17
18
19
20
21
22
23
24
25
26
27
28
29
30
31
32
33
34
35
36
37
38
39
40
41
42
43
44
45
46
47
48
49
50
51
52
53
54
55
56
57
58
59
60

TABLE OF CONTENTS GRAPHIC (TOC)

“Poly(sarcosine)-Based Nano-Objects with Multi-Protease Resistance by Aqueous Photoinitiated Polymerization-Induced Self-Assembly (Photo-PISA)”

Spyridon Varlas,^a Panagiotis G. Georgiou,^{a,b} Panayiotis Bilalis,^c Joseph R. Jones,^a Nikos Hadjichristidis,^{c} and Rachel K. O'Reilly^{a*}*



Poly(sarcosine)-based diblock copolymer nano-objects with various morphologies were prepared by combining *N*-carboxyanhydride ring-opening polymerization (ROP) and RAFT-mediated photoinitiated polymerization-induced self-assembly (photo-PISA) of a commercially available monomer (2-hydroxypropyl methacrylate), using a poly(sarcosine) macromolecular chain transfer agent. Based on a constructed phase diagram, vesicles were chosen and the resistance of both empty and horseradish peroxidase-loaded ones against degradation by a series of proteolytic enzymes was evaluated.